MOLECULAR AND CELLULAR BIOLOGY, Jan. 1999, p. 241–250 Vol. 19, No. 1
0270-7306/99/$04.00+0

The *msh2* Gene of *Schizosaccharomyces pombe* Is Involved in Mismatch Repair, Mating-Type Switching, and Meiotic Chromosome Organization

CLAUDIA RUDOLPH,[1] CHRISTOPHE KUNZ,[1] SANDRO PARISI,[1] ELISABETH LEHMANN,[1] EDGAR HARTSUIKER,[1] BERTHOLD FARTMANN,[2] WILFRIED KRAMER,[2] JÜRG KOHLI,[1] AND OLIVER FLECK[1]*

Institute of General Microbiology, University of Bern, CH-3012 Bern, Switzerland,[1] and Institute of Molecular Genetics, Georg August University Göttingen, D-37077 Göttingen, Germany[2]

Received 25 June 1998/Returned for modification 4 August 1998/Accepted 9 October 1998

We have identified in the fission yeast *Schizosaccharomyces pombe* a MutS homolog that shows highest homology to the Msh2 subgroup. *msh2* disruption gives rise to increased mitotic mutation rates and increased levels of postmeiotic segregation of genetic markers. In bandshift assays performed with *msh2*Δ cell extracts, a general mismatch-binding activity is absent. By complementation assays, we showed that *S. pombe msh2* is allelic with the previously identified *swi8* and *mut3* genes, which are involved in mating-type switching. The *swi8-137* mutant has a mutation in the *msh2* gene which causes a truncated Msh2 peptide lacking a putative DNA-binding domain. Cytological analysis revealed that during meiotic prophase of *msh2*-defective cells, chromosomal structures were frequently formed; such structures are rarely found in the wild type. Our data show that besides having a function in mismatch repair, *S. pombe msh2* is required for correct termination of copy synthesis during mating-type switching as well as for proper organization of chromosomes during meiosis.

In *Escherichia coli*, the *mutHLS* system efficiently repairs single-base mismatches except C/C, as well as small single-strand insertions and deletions (45). In addition, this system maintains genome stability by prevention of recombination between homeologous sequences (55). The MutS protein recognizes and binds to mismatches. The site-specific endonuclease MutH binds to hemimethylated *dam* (GATC) sequences. MutL connects both complexes by binding to MutS and MutH. Upon complex formation, MutH is activated and initiates excision of the newly synthesized DNA strand, followed by resynthesis, resulting in intact duplex DNA (39, 45, 46, 47).

Several MutS and MutL homologs have been identified in eukaryotes (13, 39, 47), indicating that the system is more complex than in bacteria. In *Saccharomyces cerevisiae*, three MutS homologs, designated Msh2 (56), Msh3 (49), and Msh6 (34, 43), and two MutL homologs, Mlh1 and Pms1 (40, 54), have been shown to be involved in mismatch repair of nuclear DNA. Msh2 forms a complex with Msh3 to repair loops and with Msh6 to repair single-base mismatches (2, 31, 34, 43). *msh2* mutants display increased mitotic and meiotic mutation rates (57) and instability of simple repeats (66). In addition, the major mismatch-binding activity of *S. cerevisiae* cell extracts is absent in *msh2* mutants (44). The mechanism of mismatch repair involving heterodimers of MutS and MutL homologous proteins is conserved in higher eukaryotes (reviewed in references 36, 46, 47, and 70). Defects in the human mismatch repair system give rise to increased microsatellite instability and predisposition to a common form of colon cancer (hereditary nonpolyposis colon cancer) (46, 70). Inactivation of the murine *MSH2* gene results in increased mutation rates, microsatellite instability, and cancer but has no effect on fertility (15). In contrast, *MLH1*-deficient mice and *PMS2*-deficient male mice are sterile. They show an arrest in meiosis I and abnormal chromosome synapsis, respectively (7, 16).

For the fission yeast *Schizosaccharomyces pombe*, at least two pathways of mismatch repair have been postulated based on two lines of evidence. Marker effects of G-to-C transversions observed in intragenic crosses indicate the existence of a major pathway able to repair most base mismatches except C/C and of a minor pathway able to correct C/C and other mismatches (62, 63). In band shift assays with *S. pombe* wild-type cell extracts, two mismatch-binding activities were identified (23). One activity binds to small loops and to most single-base mismatches but not C/C; the second activity binds to C/C and all other cytosine-containing mismatches. Due to its substrate specificity and excision tract length, the major pathway was proposed to be homologous to the *E. coli mutHLS* system. To differentiate the functions of the two pathways, we engaged in the isolation of genes homologous to *mutL* and *mutS*. The characterization of the *S. pombe mutL* homolog *pms1*$^+$ was described elsewhere (60). *S. pombe swi4*$^+$, the homolog of *S. cerevisiae MSH3*, was identified due to its involvement in mating-type (MT) switching (21). Here we report the isolation of the *S. pombe msh2*$^+$ gene and its involvement in mismatch repair, MT switching, and meiotic chromosome organization.

MATERIALS AND METHODS

Strains and media. All *S. pombe* strains were derived from the original wild-type strain introduced by Leupold (reviewed in reference 29) and are listed in Table 1. Standard media and general genetic methods were described by Gutz et al. (29). YEA (yeast extract agar) medium containing a limiting amount of adenine or MMA (minimal medium) with limiting adenine supplementation (5 mg/liter) was used to investigate the colony color of *ade6* mutants. Adenine limitation allows *ade6* mutants to grow, but due to the block in adenine synthesis they accumulate a red pigment (29). MMA medium used for fluctuation tests contained 200 mg of guanine per liter to inhibit background growth of adenine auxotrophs (14).

PCR, gene cloning, and physical mapping. To clone the *S. pombe msh2*$^+$ gene, we performed PCR with degenerate primers derived from amino acid sequences highly conserved among MutS proteins. The 5′ oligonucleotide 5′-GCTCTAGA CNGGNCCNAA(C/T)ATGGG-3′ was derived from the peptide motif TGPN MG (amino acids 687 to 692 in *S. cerevisiae* Msh2). The 3′ oligonucleotides

* Corresponding author. Mailing address: Institute of General Microbiology, University of Bern, Baltzerstrasse 4, CH-3012 Bern, Switzerland. Phone: (41) 31 631 4656. Fax: (41) 31 631 4684. E-mail: fleck@imb.unibe.ch.

TABLE 1. *S. pombe* strains used in this study

Strain	Genotype	Reference or source
968	h^{90}	29
972	h^-	29
34-1344	h^- *ade6-51*	Strain collection, University of Bern
57-2254	h^- *his3-D1*	10
JB6	h^+/h^- *ade6-M210/ade6-M216*	J. Bähler
E113	h^{90} *ade6-M210 his2 swi8-113*	R. Egel[a]
E120	h^{90} *ade6-M210 his2 swi8-120*	R. Egel[a]
E131	h^{90} *ade6-M210 his2 swi8-131*	R. Egel[a]
E137	h^{90} *ade6-M210 his2 swi8-137*	R. Egel[a]
HE443	h^{90} *ade6-M210 his2 swi8-2*	K. Ostermann[b]
HE447	h^{90} *ade6-M210 his2 swi8-3*	K. Ostermann[b]
HE449	h^{90} *ade6-M210 his2 swi8-4*	K. Ostermann[b]
HE460	h^{90} *ade6-M210 his2 swi8-5*	K. Ostermann[b]
HE461	h^{90} *ade6-M210 his2 swi8-6*	K. Ostermann[b]
HE468	h^{90} *ade6-M210 his2 swi8-7*	K. Ostermann[b]
HE471	h^{90} *ade6-M210 his2 swi8-8*	K. Ostermann[b]
HE474	h^{90} *ade6-M210 his2 swi8-9*	K. Ostermann[b]
HE475	h^{90} *ade6-M210 his2 swi8-10*	K. Ostermann[b]
HE480	h^{90} *ade6-M210 his2 swi8-11*	K. Ostermann[b]
MAB033	h^- *ade6-M210 his3-D1 leu1-32 ura4-aim ura4-D18*	8
MAB054	h^- *ade6-M210 his3-D1 msh2::his3*$^+$ *ura4-aim ura4-D18*	8
Ru31	h^{90} *ade6-M210 his7 swi8-137 ura4-D18*	This study[a]
Ru32	h^{90} *ade6-M210 mut3-25 ura4-D18*	This study[c]
Ru34	h^{90} *ade6-M210 lys1-131 swi8-49*	This study
Ru37	h^{90} *ade6-M210 his3-D1 ura4-D18*	This study
Ru39	h^- *his3-D1 msh2::his3*$^+$	This study
Ru108	h^+ *ade6-M210 his3-D1 msh2::his3*$^+$	This study
Ru109	h^{90} *ade6-M210 his3-D1 msh2::his3*$^+$ *ura4-D18*	This study
Ru125	h^- *ade6-51 his3-D1 msh2::his3*$^+$	This study
Ru189	h^- *ade6-M216 his3-D1 msh2::his3*$^+$	This study
Ru195	h^+ *ade6-704 his3-D1 msh2::his3*$^+$ *sup3-UGA,r36*	This study
Ru196	h^- *ade6-704 his3-D1 msh2::his3*$^+$ *sup3-UGA*	This study
Ru198	h^+/h^- *ade6-M210/ade6-M216 his3-D1/his3-D1 msh2::his3*$^+$*/msh2::his3*$^+$	This study
Ru211	h^+ *ade6-M26 his3-D1 msh2::his3*$^+$	This study
Ru260	h^{90} *ade6-M210 lys1-131 swi8-1*	This study[b]

[a] Alleles *swi8-49*, *swi8-113*, *swi8-120*, *swi8-131*, and *swi8-137* were isolated by R. Egel (Copenhagen, Denmark) after ethyl methanesulfonate mutagenesis.

[b] Alleles *swi8-1* to *swi8-11* were isolated by K. Ostermann (Braunschweig, Germany) in a two-step mutagenesis with UV irradiation and ethyl methanesulfonate treatment (22).

[c] The *mut3-25* mutant was isolated by P. Munz (Bern, Switzerland) after UV irradiation (48).

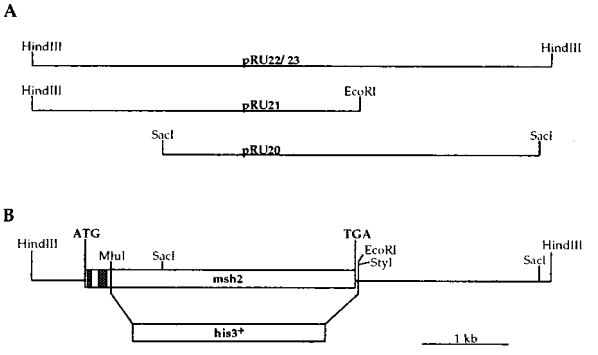

FIG. 1. Structure of the *msh2*$^+$ gene and the *msh2::his3*$^+$ insertion mutation. (A) Restriction fragments containing the *msh2*$^+$ coding region. The 4.3-kb *Sac*I fragment and the 4-kb *Hin*dIII/*Eco*RI fragment were subcloned from cosmid c24C6 (32) into pUC18, giving rise to plasmids pRU20 and pRU21, respectively, and were used for sequencing. The 6.3-kb *Hin*dIII fragment was inserted into vectors pUR19 and pBluescript KS, resulting in plasmids pRU22 and pRU23. pRU22 was used for complementation assays, while pRU23 was the basis for the *msh2::his3*$^+$ gene disruption cassette. (B) Insertion of the *his3*$^+$ marker at the *msh2* locus. The open box represents the *msh2*$^+$ coding region; dark grey boxes indicate the two introns. The *his3*$^+$ marker (light grey box) was inserted into the *Mlu*I and *Sty*I restriction sites of pRU23 as shown to give rise to plasmid pRU24. The resulting *msh2::his3*$^+$ *Hin*dIII fragment was transformed into strain 57-2254. It was also subcloned into the vector pUR19, resulting in pRU28.

5′-CACGGTACCNCGNCC(C/T)AA(C/T)TC(A/G)TC-3′ and 5′-CACGGTACC(C/T)CTNCC(C/T)AA(C/T)TC(A/G)TC-3′ were derived from the consensus sequence DELGRG (amino acids 767 to 772 in *S. cerevisiae* Msh2). An *Xba*I site in the 5′ primer and *Kpn*I sites in the 3′ primers were used for cloning of the resulting PCR fragments. PCRs were performed in 100 μl containing 250 to 500 ng of *S. pombe* genomic DNA, 200 pmol of each oligonucleotide primer, 0.1 U of Perfect Match Polymerase Enhancer (Stratagene), 1 U of *Tfl* DNA polymerase (Epicentre), 1× *Tfl* buffer, 1.5 mM $MgCl_2$, and 1.5% dimethyl sulfoxide. Reactions consisted of 35 cycles of 45 s at 94°C, 1 min at 45°C, and 1 min at 72°C. Fragments of about 270 bp in size were eluted from an agarose gel and reamplified by 25 cycles of 45 s at 94°C, 1 min at 42°C, and 1 min at 72°C. PCR products were digested with *Xba*I and *Kpn*I, cloned into M13mp18, and sequenced with universal primers. Based on the sequence of Msh2-specific inserts, the primers Msh2-inv-up (GTGTGGCATGCCGGCAATAACTCCAAC) and Msh2-inv-down (CAGTGCCTTGTGAAGTGGCTGATATCTAG) were synthesized. For inverse PCR, genomic *S. pombe* DNA was digested with *Spe*I and religated with T4 DNA ligase (Boehringer Mannheim). Using the religated *Spe*I fragments as templates, PCRs with the oligonucleotides Msh2-inv-up and Msh2-inv-down were carried out. An *Sph*I recognition site was introduced in Msh2-inv-up, an *Eco*RV recognition site was introduced in Msh2-inv-down. PCRs consisted of 35 cycles of 45 s at 94°C, 30 s at 60°C, and 3 min at 70°C, using the reaction conditions described above. Identity of the resulting 1.6-kb fragment was confirmed by sequencing the ends of cloned PCR products. A 0.8-kb *Spe*I/*Sph*I fragment of the 1.6-kb inverse-PCR fragment was used to hybridize *S. pombe* cosmid and P1 phage libraries gridded on high-density filters (32). Eighteen positive clones were obtained, and all map to the chromosome II interval between *cdc10* and *his2*.

Subcloning, nucleotide sequence analysis, and gene disruption. Restriction mapping was performed by Southern analysis of digested cosmid clone c24C6 (Fig. 1A). A 4.3-kb *Sac*I fragment and a 4-kb *Eco*RI/*Hin*dIII fragment were subcloned into pUC18, resulting in plasmids pRU20 and pRU21, respectively (Fig. 1A). A 6.3-kb *Hin*dIII fragment was cloned into pUR19 to give rise to pRU22. Nested deletions of pRU20 were obtained by exonuclease III treatment (Erase-a-Base system; Promega) and were sequenced by using either a universal or reverse M13 primer or synthesized oligonucleotides derived from internal sequences (data not shown). The sequence upstream of the internal *Sac*I site was determined by using plasmid pRU21 and synthesized oligonucleotides. Sequencing reactions on both DNA strands of *msh2*$^+$ were performed by the dideoxy-chain termination method, using a sequencing kit (United States Biochemical Sequenase kit). For sequencing the *swi8-137* mutation, PCR was performed on genomic DNA of strain E137. A fragment of about 1.9 kb containing the 5′ part of *msh2* was obtained with primers P26 (5′-TGGTGTTTAATAGTTCGAATGC-3′) and P5 (5′-CTCCTCATCAAACTCTGCACGG-3′), and an ~1.7-kb fragment containing the 3′ part of *msh2* was obtained with primers P4 (5′-CACTTCCGAAGATCGTTACGGT) and 3′msh2 (5′-CTTCCAAAAAACATGTACCTTGG-3′). For both reactions, the program consisted of an initial 5-min denaturation at 94°C, 30 cycles of 45 s 94°C, 45 s 48°C, and 2.5 min 72°C, and finally an extension step of 10 min at 72°C. The PCR products were separated from primers, and the single coding strands were amplified by 20 cycles with either primer P5 or primer 3′msh2. Sequences were determined with internal primers by the dideoxy method. From the region containing the *swi8-137* mutation, the complementary strand was also amplified and sequenced.

For gene disruption, the 6.3-kb *Hin*dIII fragment containing the *msh2*$^+$ open reading frame (ORF) and flanking sequences was cloned into pBluescript KS, resulting in pRU23. *Mlu*I and *Sty*I restriction sites at the 5′ and 3′ ends, respectively, of the *msh2*$^+$ gene were used to integrate the *his3*$^+$ marker (10). For this purpose, *Mlu*I and *Sty*I sites at the 3′ and 5′ ends, respectively, of *his3*$^+$ were introduced by PCR. By this insertion, 94% of the *msh2*$^+$ ORF was deleted (Fig. 1B). From the resulting plasmid (pRU24), the *msh2::his3*$^+$ fragment was isolated after digestion with *Pst*I and *Sal*I and used to transform the strain 57-2254. Transformation was carried out by the lithium acetate method (35). One transformant (Ru39) with the correct *msh2::his3*$^+$ gene disruption, as identified by Southern analysis (data not shown), was stored and used for all further crosses and experiments.

The *msh2::his3* fragment obtained by *Pst*I and *Sal*I digestion of pRU24 was also subcloned into the vector pUR19, resulting in plasmid pRU28. This plasmid served as control in the complementation assays.

Analysis of *msh2*$^+$ expression. A meiotic time course was performed with the diploid wild-type strain JB6 as described by Bähler et al. (6). Samples were taken before the shift to meiosis (mitotic probe) and every 2 h thereafter. Total RNA isolation and Northern analysis were performed as described elsewhere (27),

using a 0.9-kb *msh2*$^+$ fragment (data not shown) as the hybridization probe. Signals were quantified with a PhosphorImager.

Mutator phenotype and mutation rate determination. *S. pombe ade6* mutants were grown on YEA medium to visualize the red colony color. White sectors in red colonies and white colonies originate by forward mutations in genes upstream of *ade6* in the adenine pathway, by mutations in suppressor genes, or less frequently by reversion of the original *ade6* mutations. White-sectored colonies were rare in wild-type strains but occurred in the majority of colonies in *msh2*, *swi8*, and *mut3* strains.

For determination of spontaneous mutation rates, single colonies from fresh plates were used to inoculate 3 ml yeast extract liquid cultures. After growth at 30°C for 36 h, appropriate dilutions were plated on YEA to determine the total viable cell number. The remainder of the cultures was pelleted; then either the cells were plated on MMA plates containing 200 mg of guanine per liter for the selection of *ade6-51* revertants or appropriate dilutions were distributed on YEA plates containing 1 g of 5-fluoro-orotic acid per liter (26) to determine the frequency of *ura4*/*ura5* mutants. To determine the frequency of Ade$^+$ revertants, 15 cultures per experiment were used, and colonies were counted after 7 days of growth. To determine the frequency of Ura$^-$ mutants, each experiment included seven cultures, and colonies were counted after 6 days of growth. Spontaneous mutation rates were determined by the method of the median (41). To determine the mutational spectra of *msh2* and wild-type strains, Ura$^-$ mutants derived from independent cultures were crossed with *ura4* mutants to discriminate whether the mutation is located in *ura4* or *ura5* and, if it is located in *ura4*, to estimate the position of the mutated site in the *ura4* gene. The mutated site was then determined by sequencing of PCR products as described elsewhere (5).

Tetrad analysis for determination of PMS. Tetrad analysis was performed to determine the spore viability and the frequency of postmeiotic segregation (PMS) in the *msh2* background. Two pairs of parental strains, both homozygous for *msh2*::*his3*$^+$, were used. One pair was heterozygous for the *ade6-M26* marker (*ade6-M26* versus *ade6*$^+$); the second pair was heterozygous for *sup3* (*sup3-UGA* versus *sup3-UGA,r36*). *sup3-UGA* but not *sup3-UGA,r36* suppresses the *ade6-704* mutation (38). Tetrads were dissected on YEA and visually analyzed after 5 days of growth at 30°C. All spore clones from aberrant tetrads were investigated for adenine prototrophy, mating type, and ploidy to exclude tetrads unlikely to result from PMS or whole chromatid conversion (WCC) events. Only tetrads consisting of four viable spores were considered. To determine whether the ratio of PMS to WCC in different crosses was significantly changed, we used χ^2 tests with 2×2 tables. Standard deviations (SD) were calculated according to the formula $SD = [p(100 - p)/n]^{1/2}$, where p is the percentage of aberrant events and n is the total number of tetrads.

Mismatch binding assay. Mismatch-binding specificities of wild-type and *msh2* cell extracts were tested by a gel retardation assay as described by Fleck et al. (23). Approximately 50 μg of protein extracts was incubated with 40 fmol of radiolabeled oligonucleotides and with 1.6 pmol of unlabeled competitor DNA (homoduplex with the same sequence context) for 20 min at 4°C. Reactions were carried out in a mixture containing 25 mM Tris-HCl (pH 7.5), 0.5 mM dithiothreitol, 4 mM spermidine, 0.5 mM EDTA, 10% glycerol, 50 mM NaCl, 25 mM KCl, 0.01 mM $ZnCl_2$, 0.1 mM dATP, 0.1 mM dCTP, 0.1 mM dGTP, and 0.1 mM dTTP. Electrophoresis of reaction mixtures in nondenaturing gels was performed at 120 V and 4°C in 40 mM Tris-HCl (pH 7.5)–0.4 M sodium acetate–0.5 mM EDTA. Substrates and competitor DNA used for the assay are derived from the M13mp9 sequence (23).

Iodine staining. *S. pombe* strains were grown on sporulation medium (MEA) for 3 days and treated with iodine vapor. The procedure stains the spores, resulting in brown colonies (29). Homothallic (h^{90}) wild-type strains exhibit homogeneous staining, referred to as an iodine-positive phenotype. After iodine treatment, colonies of h^{90} mutants partially defective in MT switching show iodine-negative sectors in the colonies, or a mottled phenotype (28). *swi8*, *msh2*, and *mut3* mutants give rise to mottled colonies, and they frequently segregate iodine-negative, nonsporulating colonies. This phenotype is specific for mutants of class II switching genes of *S. pombe*, which are thought to be defective in the termination step of copy synthesis during MT switching (17, 20, 22, 30).

Complementation assays. *S. pombe* strains were transformed by the lithium acetate method (35) and plated onto MMA. After 7 days, transformants were replica plated onto YEA and MEA to examine complementation of the mutator phenotype and of the switching defect, respectively. For each transformation, 100 colonies were analyzed by careful visual examination. For complementation of the MT switching defect, only iodine-positive or mottled colonies, not iodine-negative colonies, were considered. The latter are due to rearrangements in the MT region which cannot be complemented (22).

Cytological procedures. To analyze the formation of linear elements in meiotic prophase, time course experiments were performed with the diploid *msh2*Δ strain Ru198 and with the diploid wild-type strain JB6. Ru198 was constructed from strains Ru108 and Ru189 by intragenic complementation of the alleles *ade6-M210* and *ade6-M216* (29). Time course experiments were performed as described by Bähler et al. (6), and samples were taken before and at hourly intervals after the shift to meiosis. To investigate the formation of linear elements, each sample was spread, silver stained, and analyzed by electron microscopy as described elsewhere (6). For each time point, 100 to 200 nuclei were examined. To monitor successful progression of meiosis, samples were treated with the DNA-staining dye 4′,6-diamidino-2-phenylindole (DAPI), and the percentage of cells containing more than one nucleus was determined by fluorescence microscopy. At least 150 cells were analyzed for each time point.

Nucleotide sequence accession number. The *S. pombe msh2* sequence has been deposited in the EMBL database under accession no. AJ006948.

RESULTS

Cloning and sequencing of *msh2*. Identification of the *S. pombe msh2* gene was based on PCR with degenerate primers as described in Materials and Methods. Screening of *S. pombe* cosmid and P1 phage libraries (32) with an *msh2*-specific probe allowed the identification of 18 clones which all mapped to the interval between *cdc10* and *his2* on chromosome II. Sequence analysis revealed an ORF of 2,949 bp, interrupted by two potential introns of 43 and 94 bp at the 5′ end (Fig. 1). PCR using a cDNA library (18) as the template and sequencing of the PCR fragments cloned into the vector pGEM3 confirmed the existence of both introns. Both contain 5′ and 3′ splice sites as well as branch sites according to the consensus sequences of Prabhala et al. (53). Intron I is located between bp 32 and 74 (with respect to the start codon) with the 5′ and 3′ splice sites GTTTGT and CAG, respectively, and the branch site CTAAT. Intron II reaches from bp 158 to 251 with the 5′ and 3′ splice sites GTAAGT and TAG, respectively, and the branch site CTAAC. The translated *msh2* ORF product consists of 982 amino acid residues which show 43% identity to *S. cerevisiae* Msh2 and human MSH2 and 28% identity to *E. coli* MutS. Amino acid sequence comparison of MutS homologs revealed that the new *S. pombe* MutS homolog belongs to the MSH2 subfamily.

To monitor expression of *S. pombe msh2* in meiosis, we performed a meiotic time course with the wild-type strain JB6. Northern analysis with RNA isolated before (mitotic cells) and at different time points after the shift to meiosis revealed two transcripts, of 2.5 and 3.2 kb (data not shown). The length of the 3.2-kb transcript corresponds well to the expected size of mRNA, while the shorter transcript might be due to an internal transcription initiation site. The level of mRNA in mitotic cells was slightly higher than the constant amount during meiosis (data not shown).

Disruption of the *msh2* gene increases spontaneous mitotic mutation rates. An *msh2*::*his3*$^+$ fragment derived from plasmid pRU24 (Fig. 1A) was used to transform strain 57-2254. For the resulting strain Ru39, correct integration of the *his3*$^+$ marker into the *msh2*$^+$ ORF was confirmed by Southern analysis (data not shown). To monitor spontaneous mitotic mutation rates in the *msh2*Δ mutant, we used two different systems. Rates of reversion from Ade$^-$ to Ade$^+$ were determined by using the *ade6-51* mutation, a C-to-T transition (62). Ade$^+$ mutants can arise due to forward mutations in suppressor genes or by reversion of the original *ade6-51* mutation. In this assay, the spontaneous mitotic mutation rate was 15-fold higher in the *msh2*Δ strain Ru125 than in the wild-type strain 34-1344 (Table 2). The forward mutation rates at *ura4*$^+$ and *ura5*$^+$ were measured for strains Ru39 and 972 as well as strains MAB033 and MAB054. In the latter two strains, the *ura4* gene is inserted about 15 kb upstream of the *ade6* gene (25). Table 2 shows that the spontaneous mitotic mutation rate for *ura4*$^+$ and *ura5*$^+$ was increased 14- to 15-fold in the *msh2*Δ mutant. We determined the nature of six mutations inactivating *ura4* in both wild-type and *msh2*Δ mutant backgrounds. In the wild-type background, five of six mutations were base substitutions (two C to T, two G to A, and one G to T); the sixth mutation was a deletion of an A at a site of two A's (A_2 to A_1). In the *msh2*Δ background, three base substitutions (two G to T and one A to G) and three one-nucleotide deletions (two T_5 to T_4 and one A_5 to A_4) were determined. These data indicate

TABLE 2. Spontaneous mitotic mutation rates

Relevant genotype	Strain	Mean forward mutation rate from Ura^+ to Ura^- ± SD[a]	Mean mutation rate from *ade6-51* to Ade^+ ± SD	Fold increase
msh2$^+$	972	$(3.7 \pm 2.3) \times 10^{-8}$		
*msh2*Δ	Ru39	$(5.2 \pm 0.45) \times 10^{-7}$		14
msh2$^+$	MAB033[b]	$(4.9 \pm 2.0) \times 10^{-8}$		
*msh2*Δ	MAB054[b]	$(7.4 \pm 4.5) \times 10^{-7}$		15
msh2$^+$	34-1344		$(3.7 \pm 0.14) \times 10^{-10}$	
*msh2*Δ	Ru125		$(5.4 \pm 0.99) \times 10^{-9}$	15

[a] SD = $[\Sigma(x - x^*)^2/n - 1]^{1/2}$, where x is the mutation rate from one experiment, x^* is the mean value, and n is the number of experiments (=2). Fluctuation tests were performed as described in Materials and Methods.
[b] The *ura4* gene is inserted about 15 kb upstream of the *ade6* gene (25). The original *ura4* gene is deleted (*ura4-D18*).

that deletion of one nucleotide in a homonucleotide run frequently occurs in *msh2*-defective cells. These deletions are likely to result from DNA strand slippage. Nevertheless, base substitutions which originated from unrepaired base-base mismatches are also accumulated in *msh2*Δ cells.

Increase of PMS and reduction of spore viability. During meiotic recombination, heteroduplex DNA is formed. When mismatch repair fails for a given marker, PMS tetrads are observed. They include $5^+:3^-$, $3^+:5^-$, or aberrant $4^+:4^-$ segregations resulting from persistence of mismatches in spores. Germination of such spores gives sectored colonies. In contrast, $6^+:2^-$ or $2^+:6^-$ gene conversions may originate from repair of mismatches in heteroduplex DNA. To investigate the ability of the *msh2*Δ mutant to repair mismatches arising during meiotic recombination, we performed tetrad analysis and determined the PMS and gene conversion frequencies with two pairs of strains. Ru195 and Ru196 are homozygous for *msh2::his3*$^+$ and heterozygous for the functional (*sup3-UGA*) and nonfunctional (*sup3-UGA,r36*) suppressor of the *ade6-704* mutation (38). Formation of heteroduplex at *sup3* gives rise to G/T and A/C mismatches. The PMS frequency in this cross was increased from 0.1% in the *msh2*$^+$ cross to 1.9% in the *msh2*Δ mutant, while the gene conversion frequency was reduced from 1.5% to 0.2% (Table 3). Therefore, the percentage of PMS events among all aberrant tetrads raised from 5.9% in the *msh2*$^+$ cross to 91% in the *msh2*Δ mutant. The second cross for determination of PMS and conversion frequencies was performed with the *msh2*Δ strains Ru39 (*ade6*$^+$) and Ru211 (*ade6-M26*). Heteroduplex DNA formed at *ade6-M26* (52, 69) results in G/A and T/C mismatches. In this cross, the PMS frequency was shifted from 0% in the wild type to 5.2% in the *msh2*Δ background, while the conversion frequency was reduced from 5.1% to 0.9%. The PMS frequency among all aberrant tetrads increased from less than 1.9% in the wild type to 85% in the *msh2*Δ mutant (Table 3). The increase in PMS frequency was highly significant for both crosses ($\chi^2 = 20.2$ for *sup3-UGA,r36*; $\chi^2 = 62.5$ for *ade6-M26*; $\chi^2_{P0.01} = 6.635$).

In addition, we determined the spore viability in both crosses. Among 3,040 spores dissected from the cross of strains Ru195 and Ru196, 2,638 (87%) were viable. Crossing strains Ru39 and Ru211 gave rise to 2,301 viable spores out of 2,684 dissected spores (86%). Thus, the overall spore lethality was about 14% in the *msh2*Δ background. For wild-type strains, an overall lethality of 3 to 8% was observed (60), indicating a two- to threefold increase of spore lethality in the *msh2*Δ mutant.

The MutS-type mismatch-binding activity is absent in *swi8-137* and *msh2*Δ cell extracts. In gel retardation assays performed with *S. pombe* wild-type cell extracts, two mismatch-binding activities were discovered (23). One low-mobility complex binds efficiently to T/G mismatches and with various efficiencies to 1-bp deletions and most single-base mismatches but not to C/C and poorly to C/A. The second, high-mobility complex binds to C/C and all other kinds of cytosine-containing mismatches.

During the screen for mutants which lack one of the mismatch-binding activities, we also tested the *swi8-137* mutant E137, which is defective in MT switching and shows a mutator phenotype (see below). As a control, we used wild-type cell extracts derived from strain 968. The wild type exhibits an activity of low mobility which specifically binds to T/G, but not to C/C or C/A, mismatches (Fig. 2, lanes 1 to 3) and therefore displays the same binding abilities as described previously (23). In contrast, this mismatch-specific activity is absent in protein extracts derived from the *swi8-137* mutant (Fig. 2, lanes 4 to 6). The C/C-binding complex is present in wild-type and *swi8-137* cell extracts. These data suggest that the low-mobility mis-

TABLE 3. PMS and gene conversion frequencies in *msh2*Δ tetrads

Relevant genotype	Conversion			PMS				Total no. of tetrads	Mean % AS[a] ± SD[b]	% PMS[c]
	$6^+:2^-$	$2^+:6^-$	%	$5^+:3^-$	$3^+:5^-$	ab4$^+$:4$^-$[d]	%			
sup3-UGA/sup3-UGA,r36										
msh2$^+$/*msh2*$^+$[e]	7	9	1.5	0	1	0	0.1	1,105	1.5 ± 0.37	5.9
*msh2*Δ/*msh2*Δ	0	1	0.2	5	5	0	1.9	514	2.1 ± 0.63	91
ade6$^+$/*ade6-M26*										
msh2$^+$/*msh2*$^+$[f]	46	6	5.1	0	0	0	0	1,018	5.1 ± 0.69	<1.9
*msh2*Δ/*msh2*Δ	3	1	0.9	15	2	3	5.2	445	6.1 ± 1.13	85

[a] AS, aberrant segregations.
[b] SD = $[p(100 - p)/n]^{1/2}$, where p is the percentage of aberrant segregations and n is the total number of tetrads analyzed.
[c] Calculated as PMS events ($5^+:3^- + 3^+:5^- + 2 \times$ ab4$^+$:4$^-$)/total number of aberrant segregations.
[d] Aberrant $4^+:4^-$ tetrads were counted as two PMS events.
[e] Data from Schär et al. (60).
[f] Data from Gutz et al. (29).

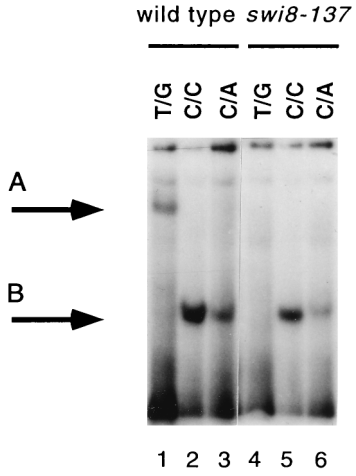

FIG. 2. Mismatch-binding activities of *S. pombe* wild-type (lanes 1 to 3) and *swi8-137* (lanes 4 to 6) cell extracts. Substrates are T/G (lanes 1 and 4), C/C (lanes 2 and 5), and C/A (lanes 3 and 6). All reactions included a 40-fold excess of unlabeled T:A competitor. The upper arrow indicates the general mismatch-binding activity; the lower arrow indicates the C/C-binding activity.

match-binding activity but not the C/C-binding activity is dependent on Swi8.

We also performed bandshift assays using the *msh2*Δ strain Ru39. With this strain, we obtained the same results as with the *swi8-137* mutant, indicating that the low-mobility complex is absent whereas binding of cytosine-containing mismatches by the high-mobility activity is unaffected (data not shown). Therefore, the low-mobility mismatch-binding complex but not the C/C-binding activity is dependent on Msh2.

The *msh2* gene is allelic with *swi8* and is involved in MT switching. *msh2* maps on chromosome II between *cdc10* and *his2*. The *swi8* gene, which is involved in MT switching, had been mapped to the same interval (30, 37). In *swi8* mutants, duplications and deletions arise in the MT region due to failure of correct termination of copy synthesis during MT switching (22). In an *ade6* background, *swi8* mutant colonies display a mutator phenotype (Materials and Methods), indicating a possible function of *swi8* in DNA repair (22). In addition the low-mobility mismatch-binding complex is absent in the *swi8-137* mutant (Fig. 2).

We supposed that *swi8* might be allelic with *msh2*. To test this possibility, we first examined whether *msh2*Δ mutant colonies show a mutator phenotype and defects in MT switching. Both phenotypes were apparent in strain Ru109. Complementation of the *swi8* defects by *msh2*$^+$ on a plasmid was then tested. For this purpose, an *swi8-137* strain (Ru31), an *msh2*Δ strain (Ru109), and a wild-type strain (Ru37) were transformed with a plasmid harboring the complete ORF of *msh2*$^+$ (pRU22 [Fig. 1A]). As controls, the same strains were transformed with the vector (pUR19) and with a plasmid containing the flanking regions of *msh2* (pRU28). In this plasmid, the *msh2::his3*$^+$ gene disruption cassette is inserted in the shuttle vector pUR19 (Fig. 1B). Transformants were replica plated onto YEA to examine the mutator phenotype and onto MEA to investigate the efficiency of MT switching. Complementation of the mutator phenotype was assayed by determination of the percentage of homogeneously red colonies versus white-sectored colonies. Transformation with *msh2*$^+$ (pRU22) resulted in 77% red colonies in the *swi8-137* mutant and 82% red colonies in the *msh2*Δ mutant (Table 4). In contrast, more than 90% sectored colonies were observed for the control transformations with the *swi8-137* and the *msh2*Δ strains. In wild-type background, about 90% of red colonies were observed in all three transformations. These data indicate that the *msh2*$^+$ gene located on plasmid pRU22 is functional and that pRU22 but none of the controls is able to complement the mutator phenotype of *swi8-137* and *msh2*Δ mutants.

TABLE 4. Complementation of the mutator phenotype

Plasmid	Colony type (%)[b]					
	*msh2*Δ[a] (Ru109)		*swi8-137* (Ru31)		Wild type (Ru37)	
	Red	White sectors	Red	White sectors	Red	White sectors
pmsh2$^+$	82	18	77	23	88	12
pmsh2Δ	1	99	1	99	90	10
pUR19	3	97	6	94	92	8

[a] Full genotypes are given in Table 1.
[b] 100 colonies per transformation were analyzed.

Complementation of the defects in MT switching was tested by determination of the percentage of iodine-positive colonies as described in Materials and Methods. The iodine-negative colonies frequently arising in *swi8* (22) and *msh2*Δ mutants were not considered. Table 5 shows that *msh2*$^+$ complements the defects of *swi8-137* and *msh2*Δ mutants, while no complementation was found for the control transformations. All wild-type colonies analyzed were iodine positive. No complementation was found with plasmid pRU28, which contains the flanking regions of *msh2*$^+$. Thus, complementation requires the *msh2*$^+$ gene and not any other genes which might be located on plasmid pRU22.

Sequencing of the *msh2* gene of the *swi8-137* mutant E137 revealed a mutation in the C-terminal part changing the CGA codon for arginine (R794) at nucleotide 2796 to a TGA stop codon (the ATG start codon is at position 280 of the sequence deposited to the EMBL database). This mutation produces a truncated Msh2 peptide without a potential DNA-binding domain (helix-turn-helix motif) and sequences highly conserved among MutS homologs (21, 49).

Genetic crosses indicated that *swi8* is allelic with *mut3* (22). The *mut3-25* mutant was isolated after methyl methanesulfonate mutagenesis and screening for mutants showing a mutator phenotype (48). Using the same assays as for the *swi8-137* mutant, we found that *msh2*$^+$ is able to complement the defects of the *mut3-25* mutant Ru32 (data not shown). Therefore, *msh2* is also allelic with *mut3*.

Our data show that *S. pombe msh2* is involved in MT switching and in mismatch repair. Both functions might be carried out by the same enzymatic activity (most likely recognition of mismatches or DNA loops), or they might be directed by different domains within the Msh2 protein. Therefore, we tested the 16 known *swi8* alleles (Table 1) for a possible separation of

TABLE 5. Complementation of defects in MT switching

Plasmid	Iodine reaction (%)[b]					
	*msh2*Δ[a] (Ru109)		*swi8-137* (Ru31)		Wild type (Ru37)	
	Positive	Mottled	Positive	Mottled	Positive	Mottled
pmsh2$^+$	95	5	96	4	100	0
pmsh2Δ	0	100	0	100	100	0
pUR19	0	100	0	100	100	0

[a] Full genotypes are given in Table 1.
[b] 100 colonies per transformation were analyzed.

function. All were isolated on the basis of defects in MT switching. We looked for *swi8* mutants displaying no mutator phenotype. No such mutant was found. In addition, the *mut3-25* allele, isolated due to its mutator phenotype (48), causes defects in MT switching (22). Therefore, no separation of function was observed among 17 *msh2* alleles.

Altered linear element formation during meiotic prophase. Involvement of mismatch repair proteins in basic mechanisms of meiosis, besides mismatch repair, has been reported for bacteria as well as for eukaryotes (reviewed in references 47 and 61). In the great majority of higher eukaryotes, a synaptonemal complex, consisting of two lateral elements (also called axial elements before formation of the complex) and a central element, is formed during meiotic prophase. In *S. pombe*, meiotic chromosome pairing and recombination do not require a synaptonemal complex. Instead, linear elements, probably corresponding to the axial elements of other eukaryotes, have been observed during meiotic prophase (reference 6 and references cited therein). In wild-type nuclei, different stages of prophase were defined by the characteristic organization of linear elements (6). Class I nuclei contain short elements and occur early in meiotic prophase. Later, the elements can form networks or bundles (class II nuclei). More abundant than class II are nuclei with long and separated filaments (class III nuclei). At the end of meiotic prophase, the elements seem to disintegrate to give rise to class I nuclei again (6).

To investigate whether *S. pombe* Msh2 is involved in meiotic prophase, we sporulated the diploid strain Ru198, homozygous for the *msh2* deletion, and as a control the diploid wild-type strain JB6. Samples were taken shortly before shift to meiotic conditions (time point zero) and at every hour after the shift. They were analyzed for completion of the first meiotic division by DAPI staining, while the formation of linear elements was monitored by spreading, silver staining, and electron microscopy of nuclei, as described by Bähler et al. (6). We observed a strong increase in the frequency of class II nuclei (Fig. 3) in the *msh2*Δ mutant, while in the wild type this class was rare: the maximum frequency of class II nuclei in the wild type was 6% (Fig. 3A, 6 h), whereas it was more than 50% in the *msh2*Δ mutant (Fig. 3B, 5 h). A concomitant decrease of class III nuclei was observed in the *msh2*Δ strain: maximum values of 39% (Fig. 3A, 6 h) in the wild type and 16% (Fig. 3B, 7 h) in the *msh2*Δ strain were observed. Examples of a wild-type class III nucleus and of a typical class II nucleus from the *msh2* mutant are shown in Fig. 4. Completion of the first meiotic division, as indicated by the amount of cells containing more than one nucleus in DAPI stains, was the same in the two strains (Fig. 3).

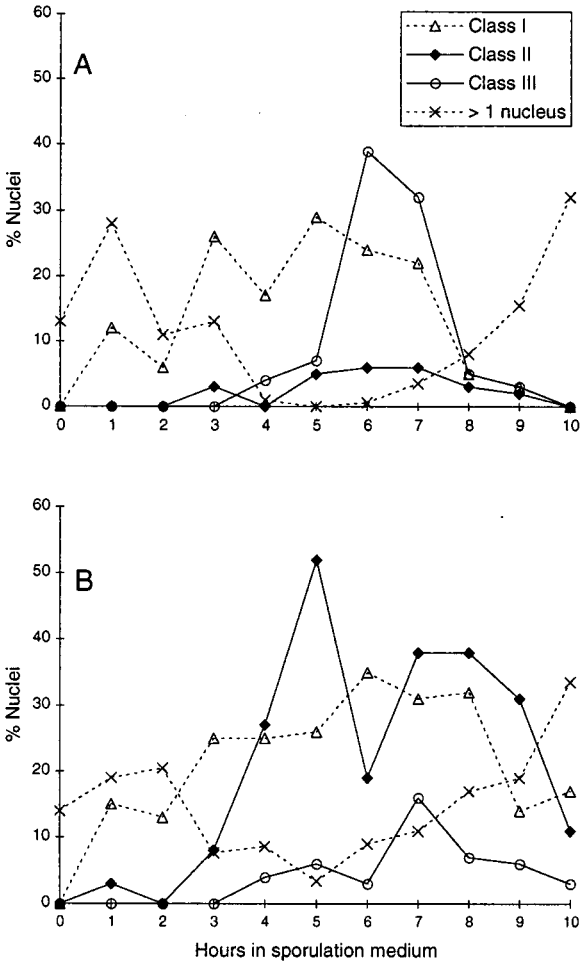

FIG. 3. Linear elements in meiotic prophase. Meiotic time courses and preparations of samples were performed with diploid wild-type strain JB6 (A) and diploid *msh2*Δ mutant Ru198 (B). After spreading and silver staining of cells from each time point, 100 to 200 nuclei were analyzed by electron microscopy to determine the percentage of each class of nuclei. To determine the percentage of cells that had completed the first meiotic division (more than one nucleus per cell), at least 150 DAPI-stained cells were analyzed for each time point.

DISCUSSION

Based on genetic data, at least two mismatch repair pathways were proposed for *S. pombe* (62, 63). Due to its substrate specificity and repair tract length, the major pathway was suggested to be homologous to the *E. coli mutHLS* system. To study the features of the two pathways in more detail, we engaged in the identification of genes that are involved in mismatch repair in *S. pombe*. The properties of the *mutL* homolog *pms1* were described recently (60). Here we report the cloning and characterization of *msh2*, a *mutS* homolog of *S. pombe*. Among the known MutS homologous proteins, Msh2 shows highest homology to the Msh2 subgroup. This and the phenotypic characterization of the *msh2*Δ strain revealed that we have identified an important component of the major mismatch repair pathway.

The *msh2* gene is involved in mitotic and meiotic mismatch repair. To investigate the function of *msh2*$^+$ in postreplicative mismatch repair, we determined mitotic mutation rates in *msh2*Δ mutants (Table 2). We found a 15-fold increase of the reversion rate of the *ade6-51* marker (a C-to-T transition). Reversions of *ade6-51* likely occur by nonrepaired base-base mismatches. The spontaneous mutation rate at *ura4*$^+$/*ura5*$^+$ was increased 14- to 15-fold. To explore the mutational spectra, we determined several *ura4* inactivating mutations from wild-type and *msh2*Δ strains. In the wild-type background, we found two C to T, two G to A, one G to T, and one A_2 to A_1. Thus, five of six analyzed mutations were base-base substitutions, while the sixth was a deletion of one A at a site of two A's. In the *msh2*Δ background, we found two G to T, one A to G, two T_5 to T_4, and one A_5 to A_4. Thus, 50% of the mutations were one-nucleotide deletions within mononucleotide runs, a type of mutation not observed in the wild type. The mutational spectra indicate that one-nucleotide loops within repeated mononucleotides occur frequently by DNA strand slippage and that Msh2 is required for their repair. Taken together, our data show that Msh2 is involved in repair of base-base mis-

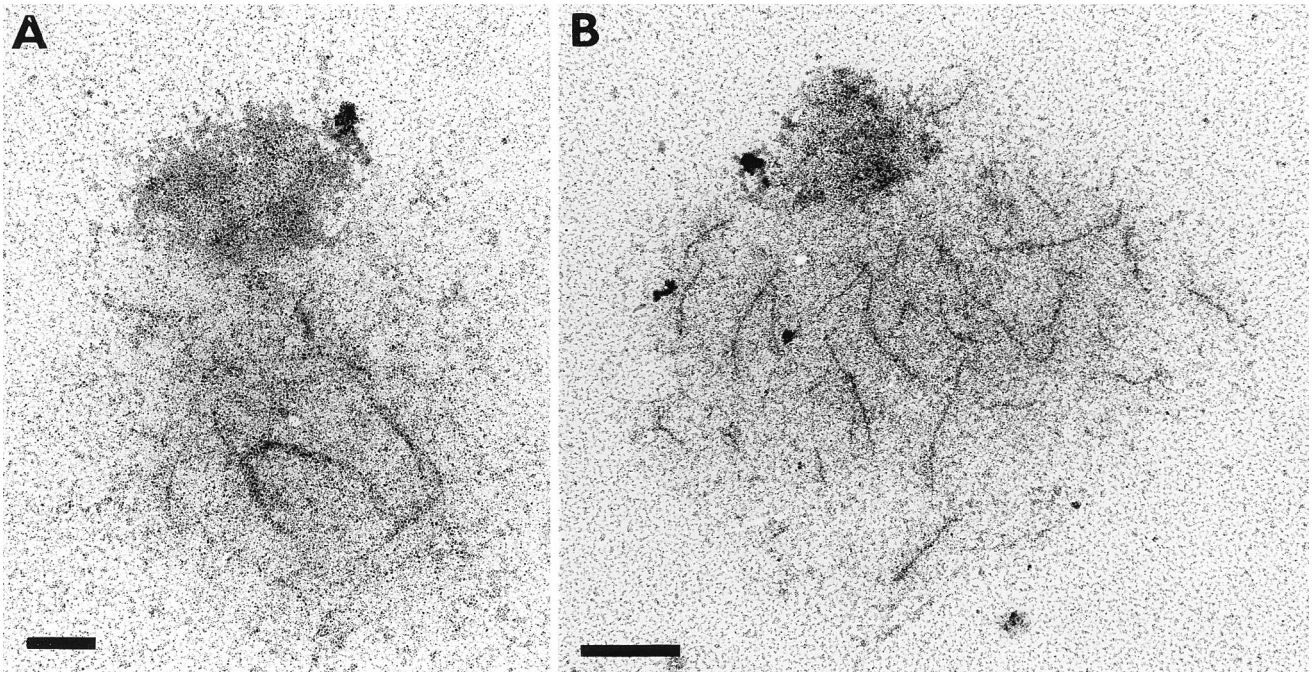

FIG. 4. (A) Example of a class II nucleus typical for the *msh2*Δ mutant. The linear elements are aggregated and form densely stained networks and bundles. This class is abundant in the *msh2*Δ mutant but rare in the wild type (see text and Fig. 3). (B) Example of class III nucleus of the wild type. Linear elements are long and separated. Class III nuclei are found frequently in wild-type cells but less often in the *msh2*Δ mutant (see text and Fig. 3). Bars represent 1 μm.

matches as well as of single unpaired nucleotides which arise during the mitotic cell cycle. Similar results were reported for Msh2 of *S. cerevisiae* (43).

Current models of meiotic recombination include the formation of heteroduplex DNA. Mismatches arise when a heteroduplex is formed between two homologous but not completely identical sequences. Mismatch repair can lead to either restoration or gene conversion, while nonrepaired mismatches give rise to PMS events. Therefore, the frequency of PMS tetrads among all aberrant tetrads is indicative of the efficiency of mismatch repair during meiosis. The frequency of all aberrant tetrads reflects the frequency of heteroduplex formation (3, 51). We used two types of crosses to determine PMS and gene conversion frequencies in the *msh2*Δ mutant. In the cross *sup3-UGA* × *sup3-UGA,r36*, the mispairs G/T and A/C can be formed; in the cross *ade6*$^+$ × *ade6-M26*, the mispairs G/A and T/C can arise. In both crosses, the PMS frequencies were significantly higher in the *msh2*Δ mutant than in the wild type (Table 3). Consistently, strongly reduced conversion frequencies were measured. Thus, the *msh2*Δ mutant is deficient in repairing mismatches in heteroduplex DNA. Interestingly, the total frequency of aberrant tetrads was not significantly altered in the *msh2*Δ mutant (Table 3). If in the wild-type background, heteroduplex DNA was repaired randomly toward wild-type or mutant information, and one half of the repair events would result in undetectable 4$^+$:4$^-$ restorations. In this case, inactivation of the mismatch repair system should increase the frequency of aberrant tetrads about twice since one half of the PMS events should then result from mismatches which if repaired would lead to restorations. In contrast, we found similar frequencies of aberrant tetrads for the *msh2*Δ mutant and for the wild type. This finding is consistent with the data reported by Schär et al. (60), who investigated PMS and gene conversion frequencies in *S. pombe pms1* mutants, and of Alani et al. (3), who studied the effects of mutated *msh2* of *S. cerevisiae*. It is concluded that mismatches in heteroduplex DNA are preferentially repaired toward gene conversion.

The *msh2* gene is involved in the major pathway of mismatch repair. The data for meiotic PMS frequencies and mitotic mutation rates show that the *msh2*$^+$ function is necessary for efficient repair of mismatches arising in meiosis and during the mitotic cell cycle. The observed increase in PMS frequencies and in mitotic mutation rates caused by *msh2*Δ is comparable to the results obtained for the *S. pombe pms1*Δ mutant (60). Formation and repair of C/C and G/G mismatches in *S. pombe* meiosis was studied according to the protocol described by Lichten et al. (42). Spore DNA isolated from wild-type strains showed no G/G mismatches, while C/C mismatches were detectable. In contrast, G/G mismatches were detected in spore DNA isolated from *msh2*Δ or *pms1*Δ mutants, while the level of C/C mismatches was comparable to the wild-type level (8). Schär et al. (60) described for the *pms1*Δ mutant a significant increase in PMS frequency when they used marker combinations giving rise to G/T and A/C or to T/C and G/A mismatches. In contrast, in crosses giving rise to C/C and G/G mismatches, the increase in PMS frequency was strikingly low, obviously because C/C repair is not carried out by the major system. These results suggest that *msh2*$^+$ and *pms1*$^+$ (60) are involved in the major but not in the minor pathway of mismatch repair in *S. pombe*.

Biochemical indication for involvement of *msh2* (*swi8*) in the major pathway of mismatch repair was obtained by bandshift assays performed with *swi8-137* and *msh2*Δ mutants. In wild-type cell extracts of *S. pombe*, two mismatch-binding activities were identified (23). One of them was concluded to be part of the major *mutLS*-like repair pathway. This binding activity, being able to bind to small insertions and deletions and to most single-base mismatches, but not to C/C, is absent in the *swi8-137* mutant. As *swi8* is allelic with *msh2*, we also tested the *msh2*Δ mutant for its mismatch-binding abilities. Like in the

swi8-137 mutant, the low-mobility activity thought to be part of the *mutLS*-like pathway is absent in *msh2*Δ cell extracts. In contrast, the mismatch-binding activity is not affected in cell extracts of a *swi4*Δ strain (23). Thus, like in other organisms (2, 24, 31, 34), Msh2, probably in a complex with Msh6, binds to base-base mismatches and small loops, while Swi4 in a complex with Msh2 binds to loops but not to base-base mismatches. The second activity, specifically binding to cytosine-containing mismatches including C/C, is still present in *msh2*Δ extracts. As the second activity was inferred to be part of the minor mismatch repair pathway, we conclude also from our biochemical data that *msh2*$^+$ is involved in the major but not the minor pathway of mismatch correction.

Involvement of *msh2* in MT switching. *swi8* mutants have been isolated according to their defects in MT switching. In homothallic strains, these defects cause a mottled colony phenotype and frequent segregation of iodine-negative colonies (17, 30). In addition, *swi8* mutants have a mutator phenotype, indicating an increased spontaneous mutation rate (22). We found the same phenotypes for the *msh2*Δ mutant. Evidence that *msh2* is allelic with *swi8* (Table 4 and 5) and also with the mutator gene *mut3* (48) was obtained from complementation assays. In these experiments, the defects in MT switching and the mutator phenotype of the *swi8-137* mutant and of the *mut3-25* mutant were complemented by *msh2*$^+$. No complementation was observed when the same strains were transformed with the vector or with a construct harboring only the flanking regions of *msh2*$^+$. These findings prompted us to conclude that complementation of the *swi8-137* and *mut3-25* defects is specifically dependent on *msh2*$^+$. That *msh2* is indeed allelic with *swi8* was proved by sequencing the *msh2* gene of the *swi8-137* mutant E137. We found a mutation near the 3′ end of the gene which creates a TGA stop codon. The truncated Msh2-137 peptide lacks the C-terminal 189 amino acids. This region contains a potential DNA-binding domain (helix-turn-helix motif) and sequences highly conserved among MutS homologs (21, 49).

Like *msh2*$^+$, *swi4*$^+$, the *S. pombe* homolog of *MSH3*, is involved in MT switching (17, 20, 21, 30). It is known from other organisms that Msh2 forms a complex with Msh3, which binds to DNA loops (1, 31, 43). MT switching in *S. pombe* is initiated at a double-strand break at the right end of *mat1* (9, 17, 50). Subsequently, copy synthesis using one of the silent cassettes (either *mat2* or *mat3*) as the template and termination at the left-flanking homology boxes H2 and H3 is thought to occur (17, 20). *swi4* and *swi8* belong to the class II of *swi* genes which are thought to be defective in termination of copy synthesis (17, 20–22). Inactivation of *swi4* or *swi8* results in frequent duplications in the MT region. It was proposed that the duplications arise when copy synthesis is not terminated in the H2 and H3 homology boxes. In consequence, intervening sequences and the next MT cassette are synthesized (17, 20). An intramolecular secondary structure in the H2 or H3 homology box which might serve as a signal for correct termination was proposed (reference 21 and Fig. 5). This stem-loop like structure containing single-stranded loops might be bound by the MutS homologous proteins Msh2 and Swi4. Also, Swi10 and Rad16, the homologs of the nucleotide excision repair proteins Rad10 and Rad1 of *S. cerevisiae*, respectively, have a function in the termination step of MT switching (11, 58). It was recently reported that *S. cerevisiae* Rad1/Rad10 and Msh2/Msh3 act in the same pathway of mitotic recombination (59, 67). It was proposed that Msh2 and Msh3 of *S. cerevisiae* bind to branched DNA structures with free 3′ tails to enable removal of nonhomologous DNA by the Rad1/Rad10 endonuclease (67). In contrast, the MutL homologous proteins Pms1 and Mlh1 have no role in this pathway. Similar functions might be required for the MT switching process of *S. pombe*. The Rad16-Swi10 endonuclease and the Msh2-Swi4 complex may act in concert on the proposed secondary structure to ensure proper resolution of a specific recombination intermediate. Msh2 and Swi4 might bind to DNA loops and/or, as proposed for *S. cerevisiae* Msh2 and Msh3, to branched DNA. Both types of DNA structures are present when the secondary structure is formed (Fig. 5). The MutL homolog Pms1 is not involved in MT switching of *S. pombe* (19). We cannot rule out the possibility that another, not yet identified MutL homolog in *S. pombe* has a function in MT switching. However, analogous to the functions of respective proteins in *S. cerevisiae*, we propose that correct termination of MT switching in *S. pombe* requires binding (by Msh2/Swi4) but not repair (mediated by MutL homologous proteins) of loop-containing and/or branched DNA structures. Binding by Msh2/Swi4 might facilitate correct termination of DNA synthesis and resolution of the intermediate carried out by the endonucleolytic activity of Rad16/Swi10.

In *swi8* mutants, a specific conversion event near the H1 box of *mat1* was also observed (22). The conversion may occur

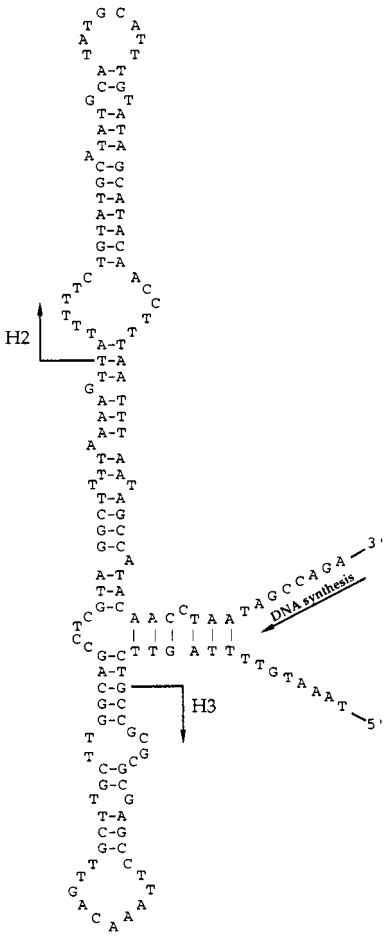

FIG. 5. Hypothetical intramolecular secondary DNA structure in the H3 and H2 homology boxes of the silent cassette *mat2*. This structure or a part of it may be formed during MT switching. Binding of the MutS homologous proteins Msh2 and Swi4 to the DNA structure may terminate copy synthesis at the template DNA strand. Only the secondary structure of the template strand is shown. A similar structure is possible in the H3 and H2 homology boxes of *mat3*. The 5′ ends of the H3 and H2 boxes are indicated.

when heteroduplex DNA formed during MT switching is extended into the region adjacent to the H1 homology box of the silent cassette *mat2*. This region shows some similarity to the corresponding region near the expression cassette *mat1*. In wild-type strains the conversion event is accurately suppressed by the *swi8*$^+$ gene product. This function is thought to be similar to the antirecombination mechanism, which prevents recombination between similar but diverged sequences (22, 55). Our data strongly support this hypothesis: *swi8* was shown to be allelic with the *mutS* homolog *msh2*, which in other organisms is known to prevent interspecies and homeologous recombination (12, 33, 55, 65).

Role of Msh2 in early meiotic prophase. During meiosis, the homologous chromosomes pair and recombine. Not much is known about the molecular mechanisms of homolog recognition, a prerequisite for proper homologous pairing and recombination. It has been demonstrated in both bacteria and eukaryotes that different mismatch repair proteins play a role in the prevention of homeologous or ectopic recombination (12, 33, 55, 65). In both yeast and mammalian cells, the suppression of homeologous recombination is Msh2 dependent (reviewed in references 47 and 61). In an *S. pombe* meiotic time course with kinetics similar to those presented in this study, stable meiotic heteroduplex DNA is detectable shortly before the first meiotic division, around 7 h after meiotic induction (8). Compared to the wild type, the *msh2*Δ mutant shows a strong increase in the amount of class II nuclei with aggregated linear elements at the expense of class III nuclei with separated linear elements. As shown in Fig. 3, the frequency of class II elements in the *msh2* mutant is higher than in the wild type after 3 h and increases to more than 50% after 5 h. Assuming that Msh2 acts on mismatches in heteroduplex DNA, this finding suggests that the protein has a role earlier in meiotic prophase before the formation of stable heteroduplex DNA, presumably by interacting with unstable heteroduplex DNA. As this heteroduplex DNA was not detected by Baur et al. (8), it might be below the detection limit of the assay. We can only speculate about the nature of this unstable heteroduplex DNA in *S. pombe* meiosis. More is known about the progression of meiotic recombination in *S. cerevisiae*: meiotic double-strand breaks appear and are resected early in meiotic prophase, before synaptonemal complex formation (68). They disappear concomitantly with the formation of double Holliday junctions, coinciding with formation of the synaptonemal complex. Double Holliday junctions persist throughout meiotic prophase and disappear when stable heteroduplex DNA is detectable and crossover products are formed (reference 68 and references cited therein). Swacha and Kleckner (68) presented a model in which mismatched base pairs are formed (and repaired) at two different time points during meiotic prophase: the first time early in meiosis, when double Holliday junctions are formed, and a second time at the end of meiosis, when the double Holliday junctions are resolved. It is likely that Msh2 binds to mismatches in heteroduplex DNA which is formed shortly before meiosis I at the end of meiotic prophase, because in tetrad analysis we observed strongly reduced repair of mismatches (Table 3). We propose that Msh2 also binds to heteroduplex DNA that is formed shortly after the initiation of meiotic recombination early in meiotic prophase, since the *msh2*Δ mutant shows an effect early in meiosis (Fig. 3 and 4). Probably *S. pombe* Msh2 has a role in the prevention of ectopic chromosome pairing. Msh2 binding may result in the rejection of heteroduplex DNA early in meiotic prophase, when the similarity or length of paired sequences is limited. A lack of Msh2 would then lead to an increase of ectopic interactions. Class II nuclei might correspond to a stage in meiotic prophase where the homology search takes place, reflected by an increase of ectopic interactions. The increased number of class II nuclei in the *msh2*Δ mutant may indicate increased and/or temporally extended pairing between homeologous sequences on nonhomologous chromosomal regions which results in an increase of ectopic interactions. This is the first indication of a possible biological role of the aggregation of linear elements in the class II nuclei and of a role of Msh2 in the homology search. It will be interesting to study the effects of *msh2*Δ on the frequency of ectopic pairing and recombination between identical and similar DNA sequences on different chromosomes in fission yeast meiosis (4, 64).

ACKNOWLEDGMENTS

We thank Primo Schär, Peter Munz, Christiane Rayssiguier, Carine Tornier, and Monika Molnar for helpful discussions, Henning Schmidt and Kai Ostermann for kindly providing the *swi8* strains, and Elmar Maier for the cosmid clones.

This work was supported by the Swiss National Science Foundation.

REFERENCES

1. **Acharya, S., T. Wilson, S. Gradia, M. F. Kane, S. Guerrette, G. T. Marsischky, R. Kolodner, and R. Fishel.** 1996. hMSH2 forms specific mispair-binding complexes with hMSH3 and hMSH6. Proc. Natl. Acad. Sci. USA **93:**13629–13634.
2. **Alani, E.** 1996. The *Saccharomyces cerevisiae* Msh2 and Msh6 proteins form a complex that specifically binds to duplex oligonucleotides containing mismatched DNA base pairs. Mol. Cell. Biol. **16:**5604–5615.
3. **Alani, E., R. A. G. Reenan, and R. D. Kolodner.** 1994. Interaction between mismatch repair and genetic recombination in *Saccharomyces cerevisiae*. Genetics **137:**19–39.
4. **Amstutz, H., P. Munz, W. D. Heyer, U. Leupold, and J. Kohli.** 1985. Concerted evolution of tRNA genes: intergenic conversion among three unlinked serine tRNA genes in *S. pombe*. Cell **40:**879–886.
5. **Ausubel, F. M., R. Brent, R. E. Kingston, D. D. Moore, J. G. Seidman, J. A. Smith, and K. Struhl (ed.).** 1987. Current protocols in molecular biology. John Wiley & Sons, Inc., New York, N.Y.
6. **Bähler, J., T. Wyler, J. Loidl, and J. Kohli.** 1993. Unusual nuclear structures in meiotic prophase of fission yeast: a cytological analysis. J. Cell Biol. **121:**241–256.
7. **Baker, S. M., C. E. Bronner, L. Zhang, A. W. Plug, M. Robatzek, G. Warren, E. A. Elliot, J. Yu, T. Ashley, N. Arnheim, R. A. Flavell, and R. M. Liskay.** 1995. Male mice defective in the DNA mismatch repair gene *PMS2* exhibit abnormal chromosome synapsis in meiosis. Cell **82:**309–319.
8. **Baur, M., P. Schär, and J. Kohli.** Unpublished data.
9. **Beach, D. H.** 1983. Cell type switching by DNA transposition in fission yeast. Nature **305:**682–687.
10. **Burke, J. D., and K. L. Gould.** 1994. Molecular cloning and characterization of the *Schizosaccharomyces pombe his3* gene for use as a selectable marker. Mol. Gen. Genet. **242:**169–176.
11. **Carr, A. M., H. Schmidt, S. Kirchhoff, W. J. Muriel, K. S. Sheldrick, D. J. Griffiths, C. N. Basmacioglu, S. Subramani, M. Clegg, A. Nasim, and A. R. Lehman.** 1994. The *rad16* gene of *Schizosaccharomyces pombe*: a homolog of the *RAD1* gene of *Saccharomyces cerevisiae*. Mol. Cell. Biol. **14:**2029–2040.
12. **Chambers, S. R., N. Hunter, E. J. Louis, and R. H. Borts.** 1996. The mismatch repair system reduces meiotic homeologous recombination and stimulates recombination-dependent chromosome loss. Mol. Cell. Biol. **16:**6110–6120.
13. **Crouse, G. F.** 1998. Mismatch repair systems in *Saccharomyces cerevisiae,* p. 411–448. In M. F. Hoekstra and J. A. Nickoloff (ed.), DNA damage and repair—biochemistry, genetics and cell biology. Humana Press, Totowa, N.J.
14. **Cummins, J. E., and J. M. Mitchison.** 1967. Adenine uptake and pool formation in the fission yeast *Schizosaccharomyces pombe*. Biochim. Biophys. Acta **136:**108–120.
15. **de Wind, N., M. Dekker, A. Berns, M. Radman, and H. te Riele.** 1995. Inactivation of the mouse *MSH2* gene results in mismatch repair deficiency, methylation tolerance, hyperrecombination, and predisposition to cancer. Cell **82:**321–330.
16. **Edelmann, W., P. E. Cohen, M. Kane, K. Lau, B. Morrow, S. Bennett, A. Umar, T. Kunkel, G. Cattoretti, R. Chaganti, J. W. Pollard, R. D. Kolodner, and R. Kucherlapati.** 1996. Meiotic pachytene arrest in *MLH1*-deficient mice. Cell **85:**1125–1134.
17. **Egel, R., D. H. Beach, and A. J. Klar.** 1984. Genes required for initiation and resolution steps of mating-type switching in fission yeast. Proc. Natl. Acad. Sci. USA **81:**3481–3485.
18. **Fikes, J. D., D. M. Becker, F. Winston, and L. Guarente.** 1990. Striking

conversion of TFIID in *Schizosaccharomyces pombe* and *Saccharomyces cerevisiae*. Nature **346:**291–294.
19. **Fleck, O.** Unpublished data.
20. **Fleck, O., L. Heim, and H. Gutz.** 1990. A mutated *swi4* gene causes duplications in the mating-type region of *Schizosaccharomyces pombe*. Curr. Genet. **18:**501–509.
21. **Fleck, O., H. Michael, and L. Heim.** 1992. The *swi4*$^+$ gene of *Schizosaccharomyces pombe* encodes a homologue of mismatch repair enzymes. Nucleic Acids Res. **20:**2271–2278.
22. **Fleck, O., C. Rudolph, A. Albrecht, A. Lorentz, P. Schär, and H. Schmidt.** 1994. The mutator gene *swi8* effects specific mutations in the mating-type region of *Schizosaccharomyces pombe*. Genetics **138:**621–632.
23. **Fleck, O., P. Schär, and J. Kohli.** 1994. Identification of two mismatch-binding activities in protein extracts of *Schizosaccharomyces pombe*. Nucleic Acids Res. **22:**5289–5295.
24. **Genschel, J., S. J. Littman, J. T. Drummond, and P. Modrich.** 1998. Isolation of MutSbeta from human cells and comparison of the mismatch repair specificities of MutSbeta and MutSalpha. J. Biol. Chem. **273:**19895–19901.
25. **Grimm, C., J. Bähler, and J. Kohli.** 1994. *M26* recombinational hotspot and physical conversion tract analysis in the *ade6* gene of *Schizosaccharomyces pombe*. Genetics **135:**41–51.
26. **Grimm, C., J. Kohli, J. Murray, and K. Maundrell.** 1988. Genetic engineering of *Schizosaccharomyces pombe*. A system for gene disruption and replacement using the *ura4* gene as selectable marker. Mol. Gen. Genet. **215:**81–86.
27. **Grimm, C., P. Schär, P. Munz, and J. Kohli.** 1991. The strong *adh* promoter stimulates mitotic and meiotic recombination at the *ade6* gene of *Schizosaccharomyces pombe*. Mol. Cell. Biol. **11:**289–298.
28. **Gutz, H., and F. J. Doe.** 1975. On homo- and heterothallism in *Schizosaccharomyces pombe*. Mycologia **67:**748–759.
29. **Gutz, H., H. Heslot, U. Leupold, and N. Loprieno.** 1974. *Schizosaccharomyces pombe*, p. 395–446. *In* R. C. King (ed.), Handbook of genetics, Vol. 1. Plenum Press, New York, N.Y.
30. **Gutz, H., and H. Schmidt.** 1985. Switching genes in *Schizosaccharomyces pombe*. Curr. Genet. **9:**325–331.
31. **Habraken, Y., P. Sung, L. Prakash, and S. Prakash.** 1996. Binding of insertion/deletion DNA mismatches by the heterodimer of yeast mismatch repair proteins MSH2 and MSH3. Curr. Biol. **6:**1185–1187.
32. **Hoheisel, J. D., E. Maier, R. Mott, L. McCarthy, A. V. Grigoriev, L. C. Schalkwyk, D. Nizetic, F. Francis, and H. Lehrach.** 1993. High resolution cosmid and P1 maps spanning the 14 Mb genome of the fission yeast *S. pombe*. Cell **73:**109–120.
33. **Hunter, N., S. R. Chambers, E. J. Louis, and R. H. Borts.** 1996. The mismatch repair system contributes to meiotic sterility in an interspecific yeast hybrid. EMBO J. **15:**1726–1733.
34. **Iaccarino, I., F. Palombo, J. Drummond, N. F. Totty, J. J. Hsuan, P. Modrich, and J. Jiricny.** 1996. MSH6, a *Saccharomyces cerevisiae* protein that binds to mismatches as a heterodimer with MSH2. Curr. Biol. **6:**484–486.
35. **Ito, H., Y. Fukuda, K. Murata, and A. Kimura.** 1983. Transformation of intact yeast cells treated with alkali cations. J. Bacteriol. **153:**163–168.
36. **Jiricny, J.** 1994. Colon cancer and DNA repair: have mismatches met their match? Trends Genet. **10:**164–168.
37. **Kohli, J., H. Hottinger, P. Munz, A. Strauss, and P. Thuriaux.** 1977. Genetic mapping in *Schizosaccharomyces pombe* by mitotic and meiotic analysis and induced haploidization. Genetics **87:**471–489.
38. **Kohli, J., P. Munz, R. Aebi, and D. Söll.** 1989. Informational suppression, transfer RNA, and intergenic conversion, p. 75–96. *In* A. Nasim, P. Young, and B. F. Johnson (ed.), Molecular biology of the fission yeast. Academic Press, Inc., New York, N.Y.
39. **Kolodner, R.** 1996. Biochemistry and genetics of eukaryotic mismatch repair. Genes Dev. **10:**1433–1442.
40. **Kramer, W., B. Kramer, M. S. Williamson, and S. Fogel.** 1989. Cloning and nucleotide sequence of the DNA mismatch repair gene *PMS1* from *Saccharomyces cerevisiae*: homology of PMS1 to procaryotic MutL and HexB. J. Bacteriol. **171:**5339–5346.
41. **Lea, D. E., and C. A. Coulson.** 1949. The distribution of the number of mutants in bacterial populations. J. Genet. **49:**264–285.
42. **Lichten, M., C. Goyon, N. P. Schultes, D. Treco, J. W. Szostak, J. E. Haber, and A. Nicolas.** 1990. Detection of heteroduplex DNA molecules among the products of *Saccharomyces cerevisiae* meiosis. Proc. Natl. Acad. Sci. USA **87:**7653–7657.
43. **Marsischky, G. T., N. Filosi, M. F. Kane, and R. Kolodner.** 1996. Redundancy of *Saccharomyces cerevisiae MSH3* and *MSH6* in *MSH2*-dependent mismatch repair. Genes Dev. **10:**407–420.
44. **Miret, J. J., M. G. Milla, and R. S. Lahue.** 1993. Characterization of a DNA mismatch-binding activity in yeast extracts. J. Biol. Chem. **268:**3507–3513.
45. **Modrich, P.** 1991. Mechanisms and biological effects of mismatch repair. Annu. Rev. Genet. **25:**229–253.
46. **Modrich, P.** 1996. Mismatch repair, genetic stability, and cancer. Science **266:**1959–1960.
47. **Modrich, P., and R. S. Lahue.** 1996. Mismatch repair in replication fidelity, genetic recombination, and cancer biology. Annu. Rev. Biochem. **65:**101–133.
48. **Munz, P.** 1975. On some properties of five mutator alleles in *Schizosaccharomyces pombe*. Mutat. Res. **29:**155–157.
49. **New, L., K. Liu, and G. F. Crouse.** 1993. The yeast gene *MSH3* defines a new class of eukaryotic MutS homologues. Mol. Gen. Genet. **239:**97–108.
50. **Nielsen, O., and R. Egel.** 1989. Mapping the double-strand breaks at the mating-type locus in fission yeast by genomic sequencing. EMBO J. **8:**269–276.
51. **Petes, T. D., R. E. Malone, and L. S. Symington.** 1991. Recombination in yeast, p. 407–521. *In* J. R. Broach, E. Jones, and J. Pringle (ed.), The molecular and cellular biology of the yeast *Saccharomyces*: genome dynamics, protein synthesis and energetics, Vol. 1. Cold Spring Harbor Press, Cold Spring Harbor, N.Y.
52. **Ponticelli, A. S., E. P. Sena, and G. R. Smith.** 1988. Genetic and physical analysis of the *M26* recombination hotspot of *Schizosaccharomyces pombe*. Genetics **119:**491–497.
53. **Prabhala, G., G. J. Rosenberg, and N. F. Käufer.** 1992. Architectural features of pre-mRNA introns in the fission yeast *Schizosaccharomyces pombe*. Yeast **8:**171–182.
54. **Prolla, T. A., D.-M. Christie, and R. M. Liskay.** 1994. Dual requirement in yeast DNA mismatch repair for *MLH1* and *PMS1*, two homologs of the bacterial *mutL* gene. Mol. Cell. Biol. **14:**407–415.
55. **Rayssiguier, C., D. S. Thaler, and M. Radman.** 1989. The barrier to recombination between *Escherichia coli* and *Salmonella typhimurium* is disrupted in mismatch-repair mutants. Nature **342:**396–401.
56. **Reenan, R. A. G., and R. D. Kolodner.** 1992. Isolation and characterization of two *Saccharomyces cerevisiae* genes encoding homologs of the bacterial HexA and MutS mismatch repair proteins. Genetics **132:**963–973.
57. **Reenan, R. A. G., and R. D. Kolodner.** 1992. Characterization of insertion mutations in the *Saccharomyces cerevisiae MSH1* and *MSH2* genes: evidence for separate mitochondrial and nuclear functions. Genetics **132:**975–985.
58. **Rödel, C., S. Kirchhoff, and H. Schmidt.** 1992. The protein sequence and some intron positions are conserved between the switching gene *swi10* of *Schizosaccharomyces pombe* and the human excision repair gene *ERCC1*. Nucleic Acids Res. **20:**6347–6353.
59. **Saparbaev, M., L. Prakash, and S. Prakash.** 1996. Requirement of mismatch repair genes *MSH2* and *MSH3* in the *RAD1-RAD10* pathway of mitotic recombination in *Saccharomyces cerevisiae*. Genetics **142:**727–736.
60. **Schär, P., M. A. Baur, C. Schneider, and J. Kohli.** 1997. Mismatch repair in *Schizosaccharomyces pombe* requires the *mutL* homologous gene *pms1*: molecular cloning and functional analysis. Genetics **146:**1275–1286.
61. **Schär, P., and J. Jiricny.** 1998. Eukaryotic mismatch repair, p. 199–247. *In* F. Eckstein and D. M. J. Lilley (ed.), Nucleic acids and molecular biology. Springer-Verlag Berlin, Heidelberg, Germany.
62. **Schär, P., and J. Kohli.** 1993. Marker effects of G to C transversions on intragenic recombination and mismatch repair in *Schizosaccharomyces pombe*. Genetics **133:**825–835.
63. **Schär, P., P. Munz, and J. Kohli.** 1993. Meiotic mismatch repair quantified on the basis of segregation patterns in *Schizosaccharomyces pombe*. Genetics **133:**815–824.
64. **Scherthan, H., J. Bähler, and J. Kohli.** 1994. Dynamics of chromosome organization and pairing during meiotic prophase in fission yeast. J. Cell Biol. **127:**273–285.
65. **Selva, E. M., L. New, G. F. Crouse, and R. S. Lahue.** 1995. Mismatch correction acts as a barrier to homeologous recombination in *Saccharomyces cerevisiae*. Genetics **139:**1175–1188.
66. **Strand, M., T. A. Prolla, R. M. Liskay, and T. D. Petes.** 1993. Destabilization of tracts of simple repetitive DNA in yeast by mutations affecting DNA mismatch repair. Nature **365:**274–276.
67. **Sugawara, N., F. Pâques, M. Colaiácovo, and J. E. Haber.** 1997. Role of *Saccharomyces cerevisiae* Msh2 and Msh3 repair proteins in double-strand break-induced recombination. Proc. Natl. Acad. Sci. USA **94:**9214–9219.
68. **Swacha, A., and N. Kleckner.** 1995. Identification of double holliday junctions as intermediates in meiotic recombination. Cell **83:**783–791.
69. **Szankasi, P., W. D. Heyer, P. Schuchert, and J. Kohli.** 1988. DNA sequence analysis of the *ade6* gene of *Schizosaccharomyces pombe*. Wild-type and mutant alleles including the recombination hot spot *ade6-M26*. J. Mol. Biol. **204:**917–925.
70. **Umar, A., and T. A. Kunkel.** 1996. DNA-replication fidelity, mismatch repair and genome instability in cancer cells. Eur. J. Biochem. **238:**297–307.